





# Multimodal imaging of the autosomal recessive spastic ataxia of Charlevoix-Saguenay phenotype

Mahmut Sami Biçimveren<sup>1</sup>, Ata Baytaroğlu<sup>2</sup>, Ali Gülen<sup>3</sup>, Fahrettin Duymuş<sup>4</sup>

<sup>1</sup>Department of Neurology, Uşak Training and Research Hospital, Uşak, Türkiye

<sup>2</sup>Department of Ophthalmology, Hacettepe University, Ankara, Türkiye

<sup>3</sup>Department of Medical Genetics, Uşak Training and Research Hospital, Uşak, Türkiye

<sup>4</sup>Department of Medical Genetics, Uşak University, Uşak, Türkiye

Autosomal recessive spastic ataxia of Charlevoix-Saguenay (ARSACS) is a rare hereditary cause of ataxia, in which the main clinical features include spastic gait, cerebellar ataxia, and sensorimotor polyneuropathy. Even in the absence of visual symptoms, grayish white retinal striations and retinal nerve fiber layer (RNFL) thickening on optical coherence tomography (OCT) can be detected in patients with ARSACS, acting as important diagnostic clues. Furthermore, sensorineural hearing loss can be detected on audiometry even in the absence of hearing complaints. Signal and volume alterations that provide important diagnostic clues for ARSACS can be identified on magnetic resonance imaging (MRI). Herein, we presented the multisystemic involvement of ARSACS through clinical findings, electroneuromyography, MRI, OCT, and audiometry.

A 28-year-old male was admitted to the neurology outpatient clinic with a complaint of gait disturbance. The patient engaged in sporting activities, including football and long jump, until 16 years of age, after which his gait progressively worsened. The patient was employed as a customer service representative. The medical history revealed no chronic illnesses, and there was no history of substance or medication use. The patient stated that he was adopted at the age of two. The biological father died when the patient was six years old; beyond this, the patient had no further information about his parents.

On neurological assessment, inspection demonstrated a spastic gait pattern, atrophy of the bilateral legs and the first dorsal interosseous muscles, as well as pes cavus deformity and hammer toe (Figure 1a). The patient was alert, oriented, and cooperative, with normal speech. Ophthalmological examination revealed best-corrected visual acuity of 20/20 in both eyes. Pupils were equal and reactive, with no relative afferent pupillary defect. Extraocular movements were full in all directions, although end-point nystagmus was observed at extreme gaze positions. Motor examination using the Medical Research Council scale revealed symmetrical findings, with strength graded as 5/5 in proximal upper limb muscles, 4/5 in distal upper limb muscles, 4/5 in proximal lower limb muscles, and 3/5 in distal lower limb muscles. Sensory testing revealed reduced vibration and light touch sensation in the distal parts of the lower extremities. Deep tendon reflexes were absent. No pathological reflexes were detected. On coordination testing, the finger to finger test revealed intention tremor and dysmetria, and dysmetria was also observed during the heel to shin test.

Electroneuromyographic assessment demonstrated findings consistent with a mixed type sensorimotor polyneuropathy, characterized by both axonal and demyelinating features (Table 1). Clinical and laboratory evaluations

**Correspondence:** Mahmut Sami Biçimveren, MD. Uşak Eğitim ve Araştırma Hastanesi, Nöroloji Kliniği, 64100 Uşak, Türkiye.

**E-mail:** bcmvrnsami@gmail.com

**Received:** February 05, 2026 **Accepted:** May 29, 2026 **Published online:** June 03, 2026

**Cite this article as:** Biçimveren MS, Baytaroğlu A, Gülen A, Duymuş F. Multimodal imaging of the autosomal recessive spastic ataxia of Charlevoix-Saguenay phenotype. Turk J Neurol 2026;32(2):191-197. <https://doi.org/10.55697/tnd.2026.655>.

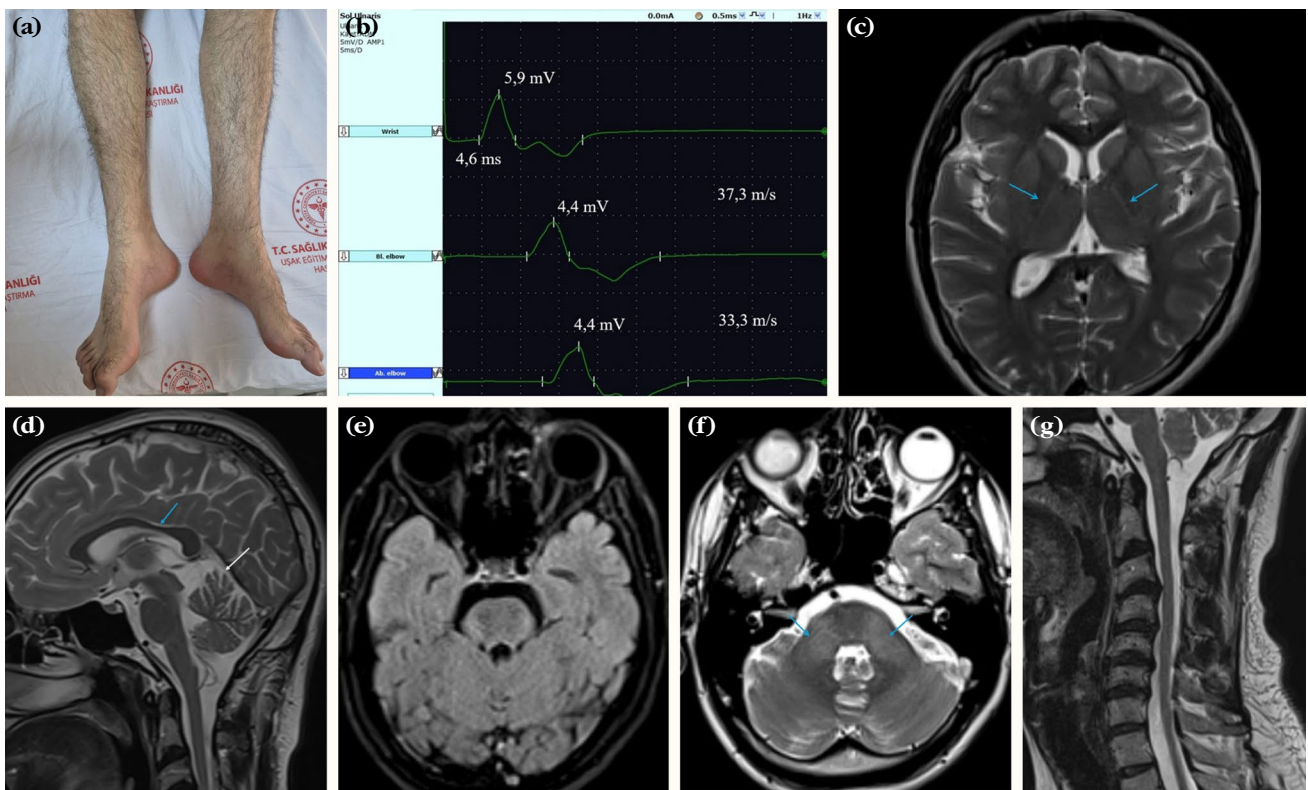


**Figure 1.** (a) Thin legs, pes cavus, and hammer toes. (b) The distal motor latency of the left ulnar nerve was prolonged (normal < 3.3 ms), with reduced compound muscle action potential amplitudes (normal  $\geq 6$  mV) and slowed conduction velocities (normal  $\geq 50$  m/s). (c) Axial T2-weighted sections demonstrate a hyperintense rim lateral to the bilateral thalami (blue arrows). (d) Sagittal T2-weighted sections demonstrate thinning of the corpus callosum (blue arrow) and superior cerebellar vermis atrophy (white arrow). (e) Axial FLAIR sections demonstrate hypointense striations within the pons. (f) Axial T2-weighted sections demonstrate hyperintensity in the bilateral middle cerebellar peduncles (blue arrows). (g) Sagittal T2-weighted sections demonstrate cervical cord atrophy.

did not demonstrate any metabolic, systemic connective tissue, or hematological disorder that could be responsible for the polyneuropathy.

Axial T2-weighted MRI revealed a hyperintense rim lateral to the bilateral thalami and bilateral hyperintensity of the middle cerebellar peduncles, and axial fluid-attenuated inversion recovery (FLAIR) sections revealed pontine hypointense striations (Figures 1c, e, f). Sagittal T2-weighted MRI revealed thinning of the corpus callosum, superior cerebellar vermis atrophy, and atrophy of the cervical spinal cord (Figures 1d, g).

Following the identification of MRI findings suggestive of ARSACS, an ophthalmology consultation was requested to evaluate the patient for retinal manifestations associated with ARSACS. The patient denied any visual symptoms, including blurred vision, transient visual obscurations, or diplopia. The anterior segment examination was unremarkable, and

intraocular pressures were normal. Dilated fundus examination showed bilateral optic disc elevation with peripapillary RNFL thickening that appeared as grayish-white striations radiating from the margins of the optic disc (Figure 2). No hemorrhages, exudates, or macular abnormalities were present.

Optical coherence tomography showed significantly increased RNFL thickness in all quadrants bilaterally, exceeding the 95<sup>th</sup> percentile of the normative database. The right eye had a mean total area thickness of 379  $\mu\text{m}$ , and the left eye measured 385  $\mu\text{m}$ , both well above the diagnostic threshold of 119  $\mu\text{m}$ . Macular structure was preserved, with minimum foveal thickness of 272  $\mu\text{m}$  in the right eye and 286  $\mu\text{m}$  in the left eye (Figure 2). Fluorescein angiography showed normal arteriovenous filling without late disc leakage, confirming the absence of true papilledema and supporting the diagnosis of RNFL hypertrophy

**TABLE 1**  
Electroneuromyographic findings

<b>Nerve conduction studies</b>											
Nerve stimulated	Stimulation site	Recording site	Amplitude; motor (mV), sensory ( $\mu$ V)			Latency (ms)			Conduction velocity (m/s)		
			R	L	N	R	L	N	R	L	N
Median (m)	Wrist	Abductor pollicis brevis	3.2	4.5	$\geq 4$	6.9	5.5	$\leq 4.2$			
Median (m)	Antecubital fossa		3.1	4					32.3	37.4	$\geq 50$
Ulnar (m)	Wrist	Abductor digiti minimi	5.2	5.9	$\geq 6$	4.6	4.6	$\leq 3.3$			
Ulnar (m)	Below elbow		3.8	4.4					37.8	37.3	$\geq 50$
Ulnar (m)	Above elbow		3.8	4.4				36.8	33.3	$\geq 50$	
Peroneal (m)	Ankle	Extensor digitorum brevis	A	A	$\geq 2$			$\leq 6.5$			
Peroneal (m)	Below fibula										$\geq 40$
Peroneal (m)	Lateral popliteal fossa									$\geq 40$	
Tibial (m)	Ankle	Abductor hallucis brevis	A	A	$\geq 4$			$\leq 5.8$			
Tibial (m)	Popliteal fossa										$\geq 40$
Median (s)	Wrist	Digit II	A	5.3	$\geq 15$		4.5	$\leq 3.5$		31.1	$\geq 50$
Ulnar (s)	Wrist	Digit V	8.4	8.4	$\geq 15$	4	3.7	$\leq 3.1$	31.9	34.3	$\geq 50$
Sural (s)	Calf	Posterior ankle	A	A	$\geq 10$			$\leq 4.4$			$\geq 40$
<b>Electromyography</b>											
Muscle	Insertional activity	Spontaneous activity			Voluntary motor unit action potentials			Activation	Recruitment		
		Fibrillation potentials	Fasciculation potentials	Intermittent potentials	Amplitude	Duration	Polyphasia				
Tibialis anterior (R)	Normal	None	None	None	$\uparrow\uparrow$	$\uparrow\uparrow$	None	Normal	$\downarrow\downarrow$		
Tibialis anterior (L)	Normal	None	None	None	$\uparrow\uparrow$	$\uparrow\uparrow$	None	Normal	$\downarrow\downarrow$		
Extensor hallucis longus (R)	Normal	None	None	None	$\uparrow\uparrow$	$\uparrow\uparrow$	None	Normal	$\downarrow\downarrow$		
Extensor hallucis longus (L)	Normal	None	None	None	$\uparrow\uparrow$	$\uparrow\uparrow$	None	Normal	$\downarrow\downarrow$		
Tibialis posterior (R)	Normal	None	None	None	$\uparrow\uparrow$	$\uparrow\uparrow$	None	Normal	$\downarrow\downarrow$		
Tibialis posterior (L)	Normal	None	None	None	$\uparrow\uparrow$	$\uparrow\uparrow$	None	Normal	$\downarrow\downarrow$		
Vastus lateralis (R)	Normal	None	None	None	$\uparrow\uparrow$	$\uparrow\uparrow$	None	Normal	$\downarrow\downarrow$		
Vastus lateralis (L)	Normal	None	None	None	$\uparrow\uparrow$	$\uparrow\uparrow$	None	Normal	$\downarrow\downarrow$		
Abductor pollicis brevis (R)	Normal	None	None	None	$\uparrow\uparrow$	$\uparrow\uparrow$	None	Normal	$\downarrow\downarrow$		
Abductor pollicis brevis (L)	Normal	None	None	None	$\uparrow\uparrow$	$\uparrow\uparrow$	None	Normal	$\downarrow\downarrow$		
First dorsal interosseous (R)	Normal	None	None	None	$\uparrow\uparrow$	$\uparrow\uparrow$	None	Normal	$\downarrow\downarrow$		
First dorsal interosseous (L)	Normal	None	None	None	$\uparrow\uparrow$	$\uparrow\uparrow$	None	Normal	$\downarrow\downarrow$		
Flexor carpi radialis (R)	Normal	None	None	None	$\uparrow\uparrow$	$\uparrow\uparrow$	None	Normal	$\downarrow\downarrow$		
Flexor carpi radialis (L)	Normal	None	None	None	$\uparrow\uparrow$	$\uparrow\uparrow$	None	Normal	$\downarrow\downarrow$		
Biceps brachii (R)	Normal	None	None	None	$\uparrow$	$\uparrow$	None	Normal	$\downarrow$		
Biceps brachii (L)	Normal	None	None	None	$\uparrow$	$\uparrow$	None	Normal	$\downarrow$		
Deltoid (R)	Normal	None	None	None	$\uparrow$	$\uparrow$	None	Normal	$\downarrow$		
Deltoid (L)	Normal	None	None	None	$\uparrow$	$\uparrow$	None	Normal	$\downarrow$		

A, absent; R, right; L, left; N, normal; m, motor; s, sensory.

rather than edema caused by elevated intracranial pressure.

Despite the absence of subjective auditory symptoms, audiometric testing identified moderate sensorineural hearing loss affecting frequencies > 4000 Hz (Figure 3).

Diagnostic whole-exome sequencing was performed, which identified a homozygous NM\_014363.6:c.4723C>T (p.Arg1575Trp) variant in the SACS (Sacsin Molecular Chaperone) gene. This allele was extremely rare in gnomAD and had not been observed in the homozygous state. Computational prediction tools indicated a deleterious effect, supported by a combined

annotation dependent depletion score of 26.5, an AlphaMissense score of 0.981, and a rare exome variant ensemble learner score of 0.785, and the substitution lied within the sacsin protein domain. ClinVar contained submissions with conflicting interpretations for this variant. We classified the variant as likely pathogenic according to American College of Medical Genetics criteria (PM1\_Supporting, PM2\_Supporting, PM3, PM5, PP3\_Moderate, and PP4). Segregation analysis could not be performed because the patient was adopted, and no biological parental samples or family history were available. Written informed consent for publication of clinical data and images was obtained from the patient.

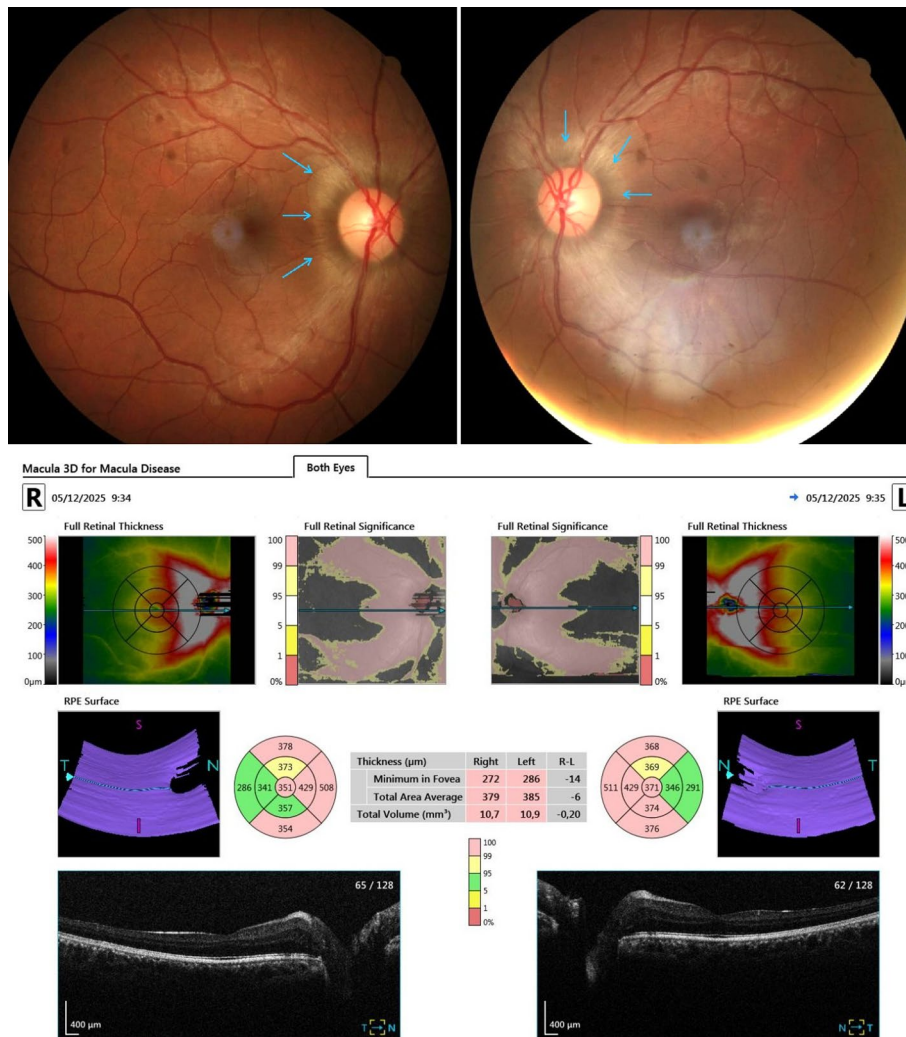


**Figure 2.** (Above) Color fundus photographs. Blue arrows denote an elevated optic disc with peripapillary RNFL thickening and grayish striations characteristic of ARSACS. (Below) Three-dimensional OCT analysis of the macula. Bilateral RNFL thickening exceeding the 95<sup>th</sup> percentile (red/yellow on significance maps). Mean total area: OD 379 µm, OS 385 µm.

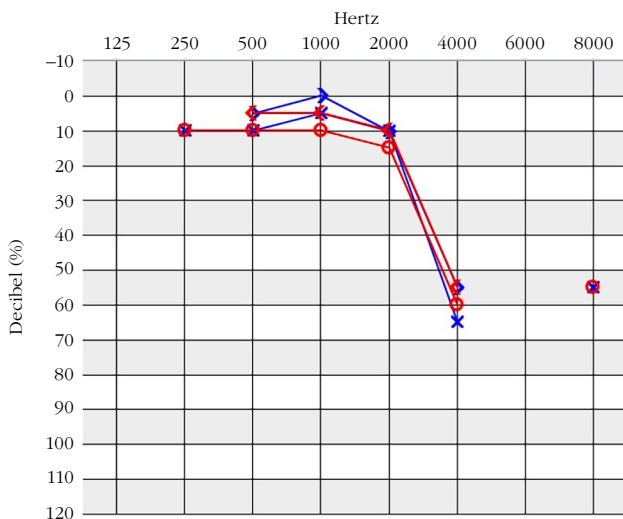


**Figure 3.** Audiometry demonstrating a moderate sensorineural hearing loss at frequencies above 4000 Hz.

Bouchard et al.<sup>[1]</sup> described ataxic patients in the Charlevoix and Saguenay regions of Quebec, Canada, who exhibited intermediate forms between Friedreich's ataxia (FA) and spastic paraplegia in 1978. Engert et al.<sup>[2]</sup> succeeded in cloning the SACS gene, which encodes the saccin protein, in 2000. The SACS gene is located at chromosome 13q12.12, and to date, more than 200 mutations have been identified in ARSACS.<sup>[3]</sup> As a result of the widespread implementation of genetic investigations, ARSACS has been reported from many regions worldwide outside Quebec.

Saccin protein interacts with heat shock proteins to regulate neurofilaments and intermediate filaments and maintain microtubule stability. In ARSACS cells, abnormal filament aggregates disrupt microtubule organization. Saccin dysfunction also impairs mitochondrial function, leading to oxidative stress, abnormal fission, and impaired autophagic function.<sup>[3]</sup>

Cerebellar ataxia, spastic gait, mixed axonal-demyelinating sensorimotor polyneuropathy, and RNFL thickening are recognized as the main clinical manifestations in ARSACS patients.<sup>[4]</sup> Nystagmus, dysarthria, and impaired smooth pursuit may be observed as additional cerebellar findings.<sup>[5]</sup> Urinary and fecal incontinence, as well as erectile dysfunction, have been reported as autonomic findings.<sup>[6]</sup> Cramps and spasms are reported in nearly 50% of patients, whereas neuropathic pain in the lower extremities is present in approximately 25%.<sup>[6]</sup> Memory impairment, concentration difficulties, hearing loss, and epilepsy have been

reported as findings beyond the main clinical features.<sup>[6]</sup> Subclinical sensorineural hearing loss at frequencies > 4000 Hz was also present in our patient.

Cerebellar atrophy, corpus callosum thinning, T2 hyperintensity in the middle cerebellar peduncles, and spinal cord atrophy on MRI can be observed in several hereditary ataxias, including spinocerebellar ataxias, FA, spastic paraplegia type 7, and ataxia telangiectasia; therefore, these findings alone are insufficient to direct the diagnosis toward ARSACS. However, as demonstrated in the MRI, the presence of pontine hypointense striations on T2 weighted sequences and a hyperintense rim lateral to the bilateral thalami are valuable diagnostic clues for ARSACS.<sup>[7]</sup>

Neuropathy is a cardinal clinical feature observed in individuals with ARSACS. Electrophysiological studies reveal, in most patients, sensorimotor neuropathy with combined demyelinating and axonal features. Motor nerve conduction velocities are reduced, in contrast to FA.<sup>[8]</sup> A moderate decrease in upper extremity motor conduction velocities was observed in our patient, consistent with a previously reported case in the literature.<sup>[9]</sup> Additionally, as observed in Charcot-Marie-Tooth disease, the nerves exhibit a symmetric and uniform slowing of conduction, while conduction block and temporal dispersion are not expected. Ultrasound examination reveals nerve enlargement in demyelinating hereditary polyneuropathies such as Charcot-Marie-Tooth disease; however, in ARSACS-related demyelinating polyneuropathy, nerve enlargement has not been observed.<sup>[10]</sup>

The pathophysiology of RNFL thickening in ARSACS remains debated. Early reports described these as hypermyelinated retinal fibers, but recent evidence suggests the thickening represents RNFL hypertrophy rather than myelination. Garcia-Martin et al.<sup>[11]</sup> proposed that SACS gene dysfunction affects nerve fiber development, causing increased RNFL density without true hypermyelination. This hypothesis is supported by the observation that tensor diffusion imaging shows hyperplasia of pontocerebellar fibers, and nerve biopsies demonstrate depletion rather than hypermyelination of nerve fibers.

Optical coherence tomography has become a vital diagnostic tool in ARSACS. Parkinson et al.,<sup>[12]</sup> in a study comparing peripapillary RNFL thickness on OCT among patients with ARSACS,

spinocerebellar ataxias, FA, other genetic ataxias (including ataxia with coenzyme Q10 deficiency, ataxia with oculomotor apraxia, episodic ataxia, ataxia associated with fibroblast growth factor mutations, fragile X-associated tremor/ataxia syndrome, and spastic paraplegia type 7), and healthy controls, reported that a mean peripapillary RNFL thickness > 119 µm on OCT provided 100% sensitivity and 99.4% specificity for distinguishing ARSACS from other ataxias, thereby representing a valuable diagnostic marker. Peripapillary RNFL thickness was markedly increased in our patient as well. We interpreted this finding as one of the most important additional biomarkers supporting the diagnosis of ARSACS among the hereditary ataxia etiologies.

The preserved visual function in our patient aligns with previous reports. Despite significant RNFL thickening, visual acuity generally remains normal in ARSACS, differentiating it from conditions such as papilledema, where prolonged disc edema results in visual field loss and eventual optic atrophy.<sup>[13]</sup> The horizontal gaze-evoked nystagmus observed reflects the underlying cerebellar pathology typical of the disease.

Ongoing experimental studies continue to explore potential treatment strategies for ARSACS. A study in mice demonstrated that mitquinol mesylate reduced cerebellar Purkinje cell degeneration by enhancing mitochondrial superoxide dismutase 2 expression.<sup>[14]</sup> The heat-shock protein 90 inhibitor KU 32 was shown to reduce neurofilament misfolding, preserve mitochondrial membrane potentials, and restore mitochondrial volume to normal levels in ARSACS cell based experiments.<sup>[15]</sup> However, no therapeutic modality is available in clinical practice that can cure the disease or decelerate the process of neurodegeneration. The efficacy of home-based speech therapy was demonstrated for speech impairment.<sup>[16]</sup> Baclofen and botulinum toxin can be used for the management of spasticity. Genetic counseling is essential for family planning, identification of carriers, and risk.

In conclusion, this report provided a detailed presentation of the ARSACS phenotype and highlighted practical clues that may facilitate its recognition by neurology practitioners.

**Data Sharing Statement:** The data that support the findings of this study are available from the corresponding author upon reasonable request.

**Author Contributions:** M.S.B.: Idea/concept, design; M.S.B., A.B., A.G., F.D.: Data collection and processing, literature review, writing the article, analysis and interpretation; M.S.B., A.B.: Materials.

**Conflict of Interest:** The authors declared no conflicts of interest with respect to the authorship and/or publication of this article.

**Funding:** The authors received no financial support for the research and/or authorship of this article.

**AI Disclosure:** The authors declare that artificial intelligence (AI) tools were not used, or were used solely for language editing, and had no role in data analysis, interpretation, or the formulation of conclusions. All scientific content, data interpretation, and conclusions are the sole responsibility of the authors. The authors further confirm that AI tools were not used to generate, fabricate, or 'hallucinate' references, and that all references have been carefully verified for accuracy.

## REFERENCES

1. Bouchard JP, Barbeau A, Bouchard R, Bouchard RW. Autosomal recessive spastic ataxia of Charlevoix-Saguenay. *Can J Neurol Sci* 1978;5:61-9.
2. Engert JC, Bérubé P, Mercier J, Doré C, Lepage P, Ge B, et al. ARSACS, a spastic ataxia common in northeastern Québec, is caused by mutations in a new gene encoding an 11.5-kb ORF. *Nat Genet* 2000;24:120-5. doi: 10.1038/72769.
3. Bagaria J, Bagyinszky E, An SSA. Genetics of Autosomal Recessive Spastic Ataxia of Charlevoix-Saguenay (ARSACS) and role of sascin in neurodegeneration. *Int J Mol Sci* 2022;23:552. doi: 10.3390/ijms23010552.
4. Rezende Filho FM, Parkinson MH, Pedrosa JL, Poh R, Faber I, Lourenço CM, et al. Clinical, ophthalmological, imaging and genetic features in Brazilian patients with ARSACS. *Parkinsonism Relat Disord* 2019;62:148-55. doi: 10.1016/j.parkreldis.2018.12.024.
5. Paulus-Andres JA, Burnett MS. Three Adult-Onset Autosomal Recessive Ataxias: What Adult Neurologists Need to Know. *Neurol Clin Pract* 2021;11:256-62. doi: 10.1212/CPJ.0000000000000947.
6. Briand MM, Rodrigue X, Lessard I, Mathieu J, Brais B, Côté I, et al. Expanding the clinical description of autosomal recessive spastic ataxia of Charlevoix-Saguenay. *J Neurol Sci* 2019;400:39-41. doi: 10.1016/j.jns.2019.03.008.
7. Biswas A, Varman M, Yoganathan S, Subhash PK, Mani S. Teaching NeuroImages: Autosomal recessive spastic ataxia of Charlevoix-Saguenay: Typical MRI findings. *Neurology* 2018;90:e1271-2. doi: 10.1212/WNL.0000000000005252.
8. Özkardes A, Turgay G, Özdağ F, Dolu H, Vural O, Yardım M. EMG and evoked responses in friedreich's ataxia. *Turk J Neurol* 1996;1:200-5.
9. García A, Criscuolo C, de Michele G, Berciano J. Neurophysiological study in a Spanish family with recessive spastic ataxia of Charlevoix-Saguenay. *Muscle Nerve* 2008;37:107-10. doi: 10.1002/mus.20878.

10. Kneer K, Straub S, Wittlinger J, Stahl JH, Winter N, Timmann D, et al. Neuropathy in ARSACS is demyelinating but without typical nerve enlargement in nerve ultrasound. *J Neurol* 2024;271:2494-502. doi: 10.1007/s00415-023-12159-2.
11. Garcia-Martin E, Pablo LE, Gazulla J, Polo V, Ferreras A, Larrosa JM. Retinal nerve fibre layer thickness in ARSACS: Myelination or hypertrophy? *Br J Ophthalmol* 2013;97:238-41. doi: 10.1136/bjophthalmol-2012-302309.
12. Parkinson MH, Bartmann AP, Clayton LMS, Nethisinghe S, Pfundt R, Chapple JP, et al. Optical coherence tomography in autosomal recessive spastic ataxia of Charlevoix-Saguenay. *Brain* 2018;141:989-99. doi: 10.1093/brain/awy028.
13. Desserre J, Devos D, Sautière BG, Debruyne P, Santorelli FM, Vuillaume I, et al. Thickening of peripapillar retinal fibers for the diagnosis of autosomal recessive spastic ataxia of Charlevoix-Saguenay. *Cerebellum* 2011;10:758-62. doi: 10.1007/s12311-011-0286-x.
14. Márquez BT, Leung TCS, Hui J, Charron F, McKinney RA, Watt AJ. A mitochondrial-targeted antioxidant (MitoQ) improves motor coordination and reduces Purkinje cell death in a mouse model of ARSACS. *Neurobiol Dis* 2023;183:106157. doi: 10.1016/j.nbd.2023.106157.
15. Nethisinghe S, Abeti R, Kesavan M, Wigley WC, Giunti P. Hsp90 Inhibition: A promising therapeutic approach for ARSACS. *Int J Mol Sci* 2021;22:11722. doi: 10.3390/ijms222111722.
16. Vogel AP, Stoll LH, Oettinger A, Rommel N, Kraus EM, Timmann D, et al. Speech treatment improves dysarthria in multisystemic ataxia: A rater-blinded, controlled pilot-study in ARSACS. *J Neurol* 2019;266:1260-6. doi: 10.1007/s00415-019-09258-4.